

MFC-structured biodegradable poly(L-lactide)/poly(butylene adipate-co-terephthalate) blends with improved mechanical and barrier properties

M. Evstatiev · S. Simeonova · K. Friedrich ·
X.-Q. Pei · P. Formanek

Received: 8 February 2013 / Accepted: 6 May 2013 / Published online: 18 May 2013
© Springer Science+Business Media New York 2013

Abstract Both polylactide (PLA) and poly(butylene adipate-co-terephthalate) (PBAT) are biodegradable polymers. They are thermoplastics which can be processed using conventional polymer processing methods. In this study, microfibrillar-reinforced composites (MFC) based on PLA/PBAT (PLA/Ecoflex[®]) blends in different weight ratios were prepared under industry-relevant conditions by melt extrusion followed by continuous cold drawing of the extrudates. Strip-like specimens (films) and plates (laminates) of the drawn blends were prepared by compression molding (CM) at processing temperature above the melting temperature (T_m) of PBAT, but below T_m of PLA. SEM and WAXS observations show that the extruded blend components are isotropic, but become highly oriented after drawing, and they are converted into MFC-structured polymer–polymer composites after CM. An effect of PLA microfibrils on the non-isothermal crystallization of the Ecoflex during cooling from the melt, associated with the formation of crystalline regions of the matrix around the fibrils, was observed. Depending on

the blend composition, the compression-molded samples possess a 3- to 7-time higher tensile strength as well as a 15–30 higher modulus than the neat Ecoflex. In addition, the MFC-structured plates exhibited superior barrier properties compared to the neat Ecoflex, e.g., the oxygen permeability decreased by up to 5 times.

Introduction

Blending is recognized as a versatile and economical method of manufacturing products able to satisfy complex performance demands [1]. However, the partners in most of the polymer blends are thermodynamically immiscible and technologically incompatible. As a result, during processing a large variety of shapes of the dispersed phase can be formed, e.g., spheres or ellipsoids or platelets [1, 2]. Which of these are actually formed depends on the weight ratio of the blend components, their chemical structure, their rheological properties, and the processing conditions. It is well known that shape and size of the dispersed phase strongly affect the properties of the final polymer blend [2]. Processing of an incompatible polymer pair in which the dispersed phase forms in situ reinforced fibers is the preferable way to achieve high mechanical properties. In order to obtain such a structure, a new type of processing route, the so-called microfibrillar-reinforced composite (MFC) concept was created about 20 years ago [3] and further developed since then [4–9]. This group of polymer/polymer composites is reinforced with bundles of polymer fibrils which possess nano- to micro-sized diameters and a high aspect ratio. A fibril can be defined as a structural entity with material properties that are biased predominantly along a linear dimension or symmetry axis [10].

The preparation of MFC includes three basic steps: (i) melt blending with extrusion of two immiscible polymers

M. Evstatiev · S. Simeonova
Laboratory on Polymers, Faculty of Chemistry, Sofia University,
1 J. Boucher Bl., 1126 Sofia, Bulgaria
e-mail: ohtme@wmail.chem.uni-sofia.bg

K. Friedrich · X.-Q. Pei (✉)
Institute for Composite Materials (IVW GmbH), Technical
University of Kaiserslautern, Erwin Schroedinger Str. 58,
67663 Kaiserslautern, Germany
e-mail: xianqiang.pei@googlemail.com

K. Friedrich
College of Engineering, King Saud University, Riyadh,
Saudi Arabia

P. Formanek
Leibniz-Institute for Polymer Research (IPF Dresden e.V.),
Dresden, Germany

having different melting temperatures T_m (*mixing step*); (ii) cold drawing of the extrudate with good orientation of the two phases (in situ *creation of polymer fibrils*); (iii) thermal treatment at a temperature between the melting temperatures of the two blend partners during different processing methods (*isotropization step*). While during the second step the two polymers are converted into a highly oriented state, i.e., one deals with an oriented (fibrillized) blend, the third step results in melting of the lower melting component and its transformation into an isotropic matrix, reinforced with the fibrils of the higher melting component. Technologically, this transition to an MFC structure can take place during processing of the drawn blend via injection- or compression molding, extrusion, or pultrusion. The essential requirement is that the processing window is not too close to the T_m of the fibrils; otherwise they will melt and return into a droplet shape. The result is a microfibril reinforced composite material with mechanical properties superior to those of the plain matrix polymer [4–9].

In the meantime other groups of investigators [11, 12] have developed similar approaches to develop in situ composites from thermoplastic polymer blends (mainly PET and polyolefins). They used means of hot stretching, but the principle is the same as mentioned before, i.e., melt extrusion, stretching, and final processing at a temperature below the melting temperature of the higher melting component.

Up to now the MFC concept was applied to blends of petroleum-based polymers such as PET, PA, PP, PE, and thermotropic liquid crystalline polymers (LCP) [4–12]. These traditional polymers exhibit a very long time of environmental decomposition, which represents a serious problem when it comes to natural degradation of plastic waste. One possibility for solution of this problem is the development of MFC materials from biodegradable polymers.

Generally, biopolymers are materials that are generated commonly from renewable natural sources. Polymers from renewable resources can be classified into three groups: (i) natural polymers, such as starch, protein, and cellulose; (ii) synthetic polymers from natural monomers, such as polylactic acids (PLAs); and (iii) polymers from microbial fermentation, such as polyhydroxybutyrates (PHBs). They can be produced by biological systems (i.e., microorganisms, plants, and animals), or chemically synthesized from biological materials (e.g., sugar, starch, natural fats and oils) [13, 14]. At present, the most important biosynthetic polymers from an overall market perspective are the polylactides, polyhydroxyalkanoates, starch and starch blends as well as cellulose derivatives [15]. Biodegradation has been defined as “an event that takes place through the action of enzymes or through chemical decomposition associated with living organisms” (e.g., bacteria, fungi) [16]. Another proposed definition is “the gradual breakdown of material mediated by specific biological activity” [17].

The main commercial route to PLA production is presently through ring-opening polymerization of L-lactide. Lactides are stereoisomers which exist in either L-, D-, meso- or racemic chiral forms, and L-lactide can be synthesized from lactic acid, obtained by fermentation of starch from agricultural feedstocks. The mechanical, thermal, and biodegradation properties of PLA are dependent on the stereosequence of the PLA repeat units. For example, PLA in which the backbone carbons have the same stereo-configuration (either R or S) is isotactic and crystallizable. The crystallinity of PLA is important for its load-bearing and gas barrier properties as well as its degradation behavior and hence its suitability for specific packaging applications [16, 17].

Beside the natural polyesters (e.g., PLAs and PHBs), it was shown that some petroleum-based synthetic co-polyesters containing aliphatic and aromatic constituents are also degraded by microorganisms. A compostable, statistical, aliphatic–aromatic co-polyester [poly(butylene adipate-co-terephthalate) (PBAT)] was commercialized by BASF (Germany) under the trade name Ecoflex[®] [18].

Both PLA and PBAT are the most common biodegradable polymers which are studied for the purpose of replacing commodity polymers in the near future. Ecoflex is a soft material with low tensile strength, high elongation, and low gas barrier properties, whereas PLA is rigid and possesses sufficient gas permeability resistance. By means of combining the two polymers through blending, it can be expected that improved physical properties and a better barrier quality can be achieved [19].

In general, several techniques can be used to improve the barrier properties of a polymer: (i) combining multiple polymer layers in a single film; (ii) coating low barrier polymers with higher barrier materials; and (iii) filling low barrier polymers with inorganic platelets or lamellae, spheres or fibers of a high barrier polymer [20]. For the last technique, the choice of the second polymer influences the mechanical (as well as the barrier) properties of the base polymer and has thus the potential to provide multiple benefits. However, these benefits depend upon several factors, including the shape and size of the reinforcing phase and its orientation relative to the direction of permeation.

An experimental design method has been used by Fakirov and others to examine the effects of several of the MFC manufacturing parameters on the final barrier properties of composite films. LLDPE/PET films were manufactured at a ratio of 70/30 (wt%) using various combinations of processing conditions (die diameter and drawing ratio), cooling conditions and microfibril orientation. The full details of the experimental design and film production parameters are given in [7, 8, 21].

A number of detailed reviews concerning the manufacturing, rheology, processing and structure–property

relationships of PLA/PBAT blends as well as mixtures of them modified with different sorts of organic or nonorganic nanoparticles and fibers have been undertaken over the past decade [9, 22–32]. Several important relationships between the morphological structure and the physical properties of such blends were established. But so far, no information on self-assembled (i.e., MFC-structured) PLA/PBAT blends could be found. As a result, the main topic of this work was formulated, namely the preparation of MFC-structured materials with improve mechanical and barrier properties based on PLA/PBAT (PLA/Ecoflex) blends. In particular, the following tasks should be solved: (i) manufacturing of fibrillized PLA/PBAT blends with different weight ratios under industrially relevant conditions; (ii) processing of strip-like specimens and plates by compression molding of the drawn blend bristles; and (iii) study of the structure–physical property relationships of these materials.

Experimental

Materials

The commercial grade PLA (Natureworks PLA 6202D) was supplied by NatureWorks[®], USA. It has a specific gravity of 1.25 g/cm³, a glass transition temperature at about 60 °C, a melting range of 160–170 °C [differential scanning calorimeter (DSC) analysis], and a melt index of 25 g/10 min (210 °C/2.16 kg) [33]. The poly(butylene adipate-*co*-terephthalate) (PBAT), grade Ecoflex[®] F Blend A1200, BASF, Germany, possesses a density of 1.26 g/cm³, a melt index of 3.5 g/10 min (190 °C/2.16 kg), and a glass transition and melting temperature of about –30 and 110–120 °C (DSC analysis), respectively [19]. Both polymers were supplied in pellet form and used as-received.

Blends and sample preparation

After drying the PLA and Ecoflex pellets at 70 °C for 24 h the polymers were tumble mixed in weight ratios of 20/80, 30/70, 40/60, and 50/50, respectively. The mixtures were melt blended on a twin-screw extruder (PL 2000 of Brabender[®] GmbH & Co. KG, Duisburg, Germany). The temperature profiles, starting from the feeding zone to the die, were 150, 180, 190, and 195 °C. The screws rotation rate was maintained at 30 rpm for all runs. After cooling of the extrudates (circular strands with a diameter of 2.2–2.6 mm) to about 45 °C, the cylindrical bristles were pressed between two rolls. In this way continuous rectangular tapes with about 1.2 mm thickness and 3.5–3.8 mm width were obtained. After roll pressing, the tapes passed through a hot chamber in which the temperature was kept at about 70 °C (above T_g of the both polymers). Here they were

continuously drawn (through neck formation) by means of a take-up device. The drawn films possessed a thickness of about 0.6–0.8 mm and a width of 1.5–1.8 mm, which corresponds to a draw ratio of 4.5–5 (when compared with the roll pressed tapes). For comparison, at the same processing window drawn PLA bristle was prepared, too. These experiments were done on an industrially relevant drawing line, existing at the Institute for Composite Materials (IVW), Kaiserslautern, Germany (Fig. 1).

The isotropization step of MFC preparation [melting of the Ecoflex and its transformation into an isotropic matrix reinforced with the fibrils of the higher melting component (PLA)] was realized by compression molding (CM) of the oriented blends on a laboratory Paul Weber hot press under the following processing conditions: temperature of the plates 140 °C (i.e., below the T_m of PLA, but above the T_m of Ecoflex), load 1.0 kN, and time under pressure 30 s. In this way strip-like samples (films) being about 0.2–0.35 mm thick and 2.5–3.2 mm wide (depending of the blend composition) were prepared. For comparison of the mechanical properties, neat PLA strip-like samples were produced under the same processing conditions as used for the drawn blends.

By means of compression molding, two layers of the oriented blend filaments were composed to form a thin unidirectionally oriented laminate (plate) with the dimensions 0.7 × 100 × 150 mm³, using the same hot press as before. The useful processing conditions were: temperature 140 °C, pressure 5 MPa, time under pressure 5 min. After melting the Ecoflex in the blends and consolidation of the individual drawn films in the mold, the resulting plates were cooled down to room temperature with a cooling rate of about 10 °C/min. Plates of the neat Ecoflex and the neat PLA were also prepared by CM at the same processing pressure and duration but at different temperatures: 140 °C for Ecoflex and 195 °C for PLA. For preparation of samples for mechanical tests, the plates were cut by means of a diamond saw into flexural bars of the size 0.7 × 10 × 100 mm³. From them “dog-bone” samples were prepared (Fig. 2).

Characterization techniques

The morphological structure of the neat polymers and the PLA/Ecoflex blends was investigated by means of scanning electron microscopy (SEM) and wide-angle X-ray scattering (WAXS). SEM observations were performed with a JEOL JSM 5400 SEM at an acceleration voltage of 10 kV. Samples from the various manufacturing and processing stages of MFC were immersed in liquid nitrogen and fractured in order to study their morphology on the respective fracture surfaces. Another set of specimens was prepared by peeling small strips from the drawn films or CM samples in the direction of the reinforcing elements.

Fig. 1 Skeleton sketch of the MFC production line

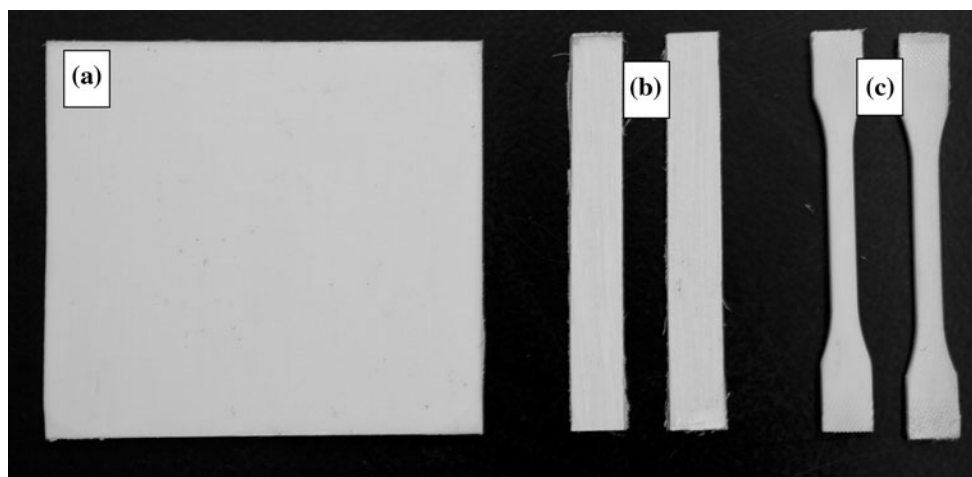
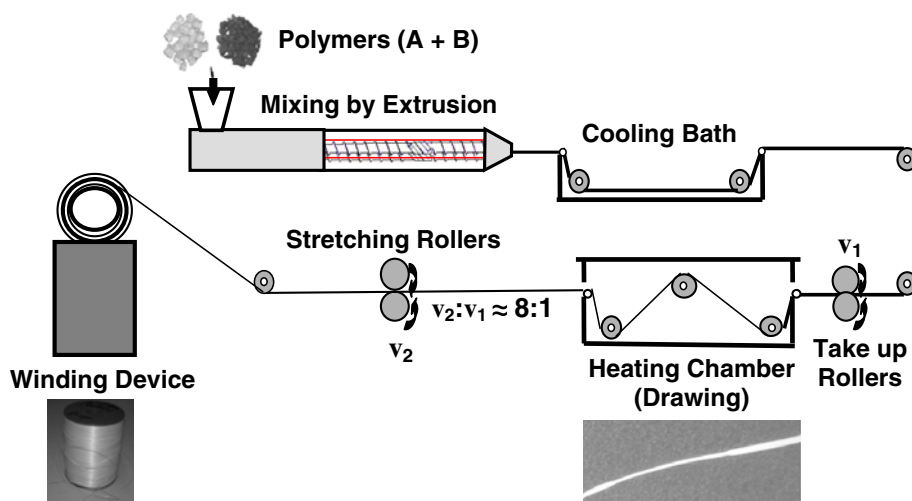


Fig. 2 The road for preparation of samples for tensile test **a** compression-molded plate, **b** cuted bars, and **c** “dog-bone” standard bars

All specimens were coated with a thin gold layer prior to SEM analysis.

Thin sections (~80 nm) for transmission electron microscopy (TEM) were prepared at -80 °C using a Leica UC6/FC6 ultramicrotome and DiATOME diamond knives. The specimens were stained in RuO₄ overnight prior to cutting and additionally for two hours after cutting. The images were recorded in a Zeiss Libra200 TEM.

WAXS patterns of the blends were obtained using a Siemens D 500 X-ray apparatus. Diffraction patterns as well as diffractograms were registered between 2θ = 10° and 35°. Informations about molecular orientation and crystallization phenomena during the various stages of blend treatment (extrusion, drawing, and compression molding) were obtained in this way.

Thermo-physical properties of the samples were measured with a differential scanning calorimeter of the type DSC 821 Mettler Toledo (Mettler Instruments GmbH, Giessen, Switzerland). The samples were crimped into aluminum pans to a total weight of 6–8 mg. All specimens

were heated to 180 °C with 10 °C/min rate in dry nitrogen atmosphere and kept there for 2 min in order to erase any previous thermal history. Then they were cooled down to room temperature at 10 °C/min rate. From the thermograms, the glass transition (*T_g*), melting (*T_m*), and crystallization (*T_c*) temperatures as well as the melting (ΔH_m) and crystallization (ΔH_c) enthalpy were recorded. The values calculated for both heats are in J/g units. A correction for diluent effects linked to the PLA incorporation into the Ecoflex matrix is shown in Eqs. 1 and 2, where *v* is the polymer weight fraction in the blend (0.25, 0.3, 0.4, 0.5 for the PLA and 0.75, 0.7, 0.6, 0.5 for the Ecoflex component, respectively).

$$\Delta H'_c = \Delta H_c / (1 - v) \tag{1}$$

and

$$\Delta H'_m = \Delta H_m / (1 - v) \tag{2}$$

The degrees of crystallinity of the neat polymers and the blends were calculated with Eq. 3:

$$W_c(\%) = (\Delta H'_m - \Delta H'_c) / \Delta H_0 \times 100\%, \quad (3)$$

where $\Delta H'_m$ is the corrected melting enthalpy, $\Delta H'_c$ is the corrected cold crystallization enthalpy, and ΔH_0 is the heat of fusion of 100 % crystalline PLA and Ecoflex, which were taken as 93 J/g [33] and 114 J/g [34], respectively.

Artificial aging of the compression-molded strip-like samples was performed in a XENOTEST ALPHA-LM chamber (Heraeus Instruments, Germany) under the following conditions: 50 W/m² ultraviolet irradiance ($\lambda = 350$ nm), relative humidity 50 %, chamber temperature 50 °C, and a duration of 10, 20, or 30 days (240, 480, and 720 h), which corresponds to irradiation doses of 4.3, 8.6, or 12.9 MJ/m², respectively.

Tensile tests of the extruded, drawn, and compression-molded samples (films and plates) were performed according to DIN 527 standard at room temperature and a crosshead speed of 50 mm/min, using a Zwick 1474 testing machine. The Young's modulus E (by the use of an incremental extensometer), the tensile strength (σ), and the strain at break (ϵ) were determined from the load–extension curves. All the data presented correspond to an average of seven measurements.

The values of E and σ as a function of blend composition are obtained according to the expression given in Eqs. 4 and 5:

$$E_{av} = E^{PLA} V^{PLA} + E^{Ecoflex} (1 - V^{PLA}) \quad (4)$$

and

$$\sigma_{av} = \sigma^{PLA} V^{PLA} + \sigma^{Ecoflex} (1 - V^{PLA}), \quad (5)$$

where E^{PLA} and σ^{PLA} are the Young modulus and the tensile strength of the PLA after drawing and hot pressing (as obtained in the present study), while $E^{Ecoflex}$ and $\sigma^{Ecoflex}$ are the modulus and strength of the CM isotropic Ecoflex. The volume fractions of PLA in the blends were calculated using a density value of 1.25 kg/m³ [33], and a density of 1.26 kg/m³ [19] was used for the Ecoflex component.

Microhardness properties of compression-molded neat polymers and PLA/Ecoflex compression-molded specimens were measured at room temperature (23 °C) using a Leica tester equipment with a square-based diamond indenter. The microhardness values (in MPa) were derived from the remaining projected indentation area according to expression 6:

$$H = k(P/d^2) \quad (6)$$

where d is the length of the impression diagonal (in meter), P the contact load applied (in N), and k a geometric factor equal to 1.854. A loading cycle of 0.4 min and loads of 1 and 2 N were used. Measurements from 10 indentations were averaged for each point of the compression-molded samples.

The oxygen transmission rate of plain Ecoflex and PLA as well as PLA/Ecoflex (25/75 and 50/50 wt%)

compression-molded plates were determinate according to ISO 15105-2, Annex A standard at 23 °C and 50 % humidity. All the data presented correspond to an average value of the measurements achieved with three different plates.

Results and discussion

X-ray analysis

Crystallization of PLA is determined by its chain regularity and mobility. As lactic acid is chiral, regularity of PLA chains is significantly affected by the ratio of the L over the D component, leading to a suppression of crystallization when a small fraction of D is present in most L chains. In general, PLA is a slowly crystallizing polymer, similar to PET. When crystallized slowly from an un-nucleated state, PLA generally becomes opaque as a result of light scattering due to the formation of large crystallites.

It is noteworthy that poly(butylene adipate-co-terephthalate) (Ecoflex) is a random copolymer; furthermore, the molar ratio of its co-monomers is around 1:1. The average block length of co-monomers in such kind of a copolymer is close to 2–3, generally too short to form regular crystalline packing, or at least the degree of crystallinity will be quite low in case it manages to crystallize at all [34, 35].

Quality trends in changing of the super molecular organization and the morphology during processing of the neat PLA, Ecoflex and their blend partners can be observed in wide-angle X-ray diffraction and SEM. Figure 3 presents the X-ray patterns obtained from a 50/50 (by wt) PLA/Ecoflex compositions after extrusion, after drawing, and after hot pressing at 140 °C, respectively. In the as-extruded state the blend components exhibit complete iso-intensity Debye rings for the Ecoflex and an amorphous halo for the PLA, i.e., the blend partners possess an isotropic distribution. The crystalline reflection arises only from the Ecoflex fraction of the blends (Fig. 3a). It should be mentioned here that the unit cell dimensions of Ecoflex are similar to that of PBT [35]. Thus it is plausible to speculate that the crystal structure of Ecoflex was formed by the butylene terephthalate (BT) units, whereas the butylene adipate (BA) units were excluded from the crystalline domains.

After drawing the isotropic distribution of the blend partners are converted into a rather perfect uni-axial orientation of the blend partners, with molecular chains strongly aligned along the stretch direction (Fig. 3b). The formation of a crystalline phase of PLA is observed too. This phenomenon is due to the stress-induced crystallization of the blend partner, arising during drawing.

PLA was found to exhibit four crystalline structures: α , β , γ , and stereo-complex [36]. The orthorhombic α crystal

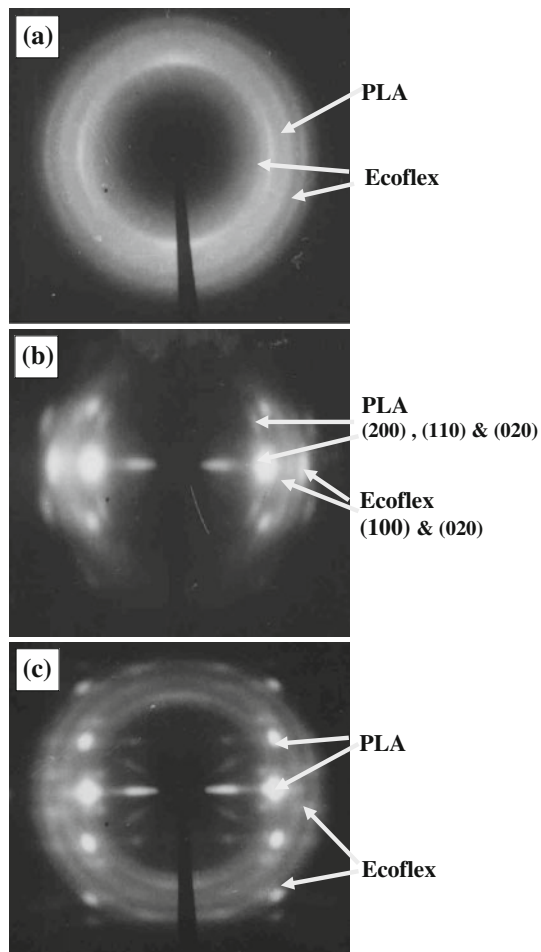


Fig. 3 X-ray patterns obtained from PLA/Ecoflex (50/50 by wt) blend after **a** extrusion, **b** drawing, and **c** compression molding

structure is the most commonly observed structure, in which the chains are in a left helical conformation. The cell dimension of the crystals vary slightly, as: $\alpha = 10.34\text{--}10.7 \text{ \AA}$, $b = 5.97\text{--}6.45 \text{ \AA}$, $c = 27.8\text{--}28.8 \text{ \AA}$. Under high stress, a β crystal orthorhombic structure ($\alpha = 10.31 \text{ \AA}$, $b = 6.1 \text{ \AA}$, $c = 9 \text{ \AA}$) with chains exhibiting more extended 3/1 helical conformation can be formed. The β crystals are found to transform into α crystals when annealed above T_g [37]. The triclinic stereo-complex can only be obtained with a 1:1 mixture of PLLA and PDLA [38].

Concerning the molecular organization of the PLA fibrils, Cicero et al. [39] investigated the crystalline morphology of PLA fibers by X-ray diffraction and atomic force microscopy. Drawing causes orientation of molecular chains, and then crystallization sets in where the microfibrils are aligned along the fiber axis during drawing. A representation of the molecular structure of PLA was proposed where the alignment of microfibrils along the fiber axis is determined by the draw ratio. As the growth

ratio increases, the tendency of microfibrils to align along the fiber axis increases. The crystalline and amorphous regions form stacks within the microfibrils and the interfibrillar regions are populated by amorphous chains [39].

After hot pressing at $140 \text{ }^\circ\text{C}$, i.e., above the T_m of Ecoflex, a completely different blend structure is created (Fig. 3c). The PLA fibrils in the blends practically preserve their orientation, as evidenced from their $kh0$ spots being situated on the equator. At the same time one can see from Fig. 3b, c that the sizes of these spots are smaller than those in the case of drawn samples. This observation indicates an improved end size perfection of the PLA crystallites which can be attributed to the additional isothermal thermal treatment during the compression molding process. At this condition the Ecoflex component in the blends under consideration are converted into an isotropic and relaxed semi-crystalline matrix reinforced with PLA fibrils (Fig. 3c).

After a more detailed analysis of Fig. 3 one can see that WAXS patterns taken at room temperature after hot pressing (Fig. 3c) are quite different from the foregoing ones (Fig. 3b) regarding the Ecoflex reflections. As a result of the non-isothermal crystallization during cooling, one has to expect the formation of a more or less isotropic and crystalline Ecoflex phase, taking into account the fact that this polymer is supposed to possess an orientation before cooling. Surprisingly enough, the distribution of Ecoflex reflections is rearranged, as can be concluded from the comparison of Fig. 3c. The displacement of reflections after crystallization shows that the chain axis of Ecoflex in the crystallites is tilted with respect to the equator direction, i.e., they are no longer parallel to the original drawing direction, as it exists in the initial drawn blend (Fig. 3c). In other words, one deals in the present case with a transcrystallization in which changes of the orientation have occurred relative to the original orientation.

Such transcrystallization can obviously take place when the PLA microfibrils play the role of a nucleating agent, similarly to various reinforcing fibers in common polymer composites. The significant difference between the two cases—the classical composites and MFC-structured ones—is that in the second case the PLA fibrils not only promote the crystallization, but they also affect the orientation of the matrix chains during the transcrystallization in such a way that they are not placed any more parallel to the chain direction of the PLA drawn phase, as well as their own orientation direction before melting during compression molding. In fact, similar transcrystallization effects of the matrix polymer onto the surface of the dispersed microfibrils have also been reported for both polyethylene terephthalate PET/nylon 12 (PA 12), polypropylene (PP)/PET, and low density polyethylene (LDPE/PET) MFCs [6, 7, 40].

Figure 4 shows the WAXS diffractograms (on transition equatorial mode) of the neat polymers and the PLA/Ecoflex 50/50 (by wt) blend after mixing, drawing, and compression molding. The pure PLLA presents one sharp peak in the 2θ range of 16.6° and a very weak one in the 2θ range of 27.5° (Fig. 4a). The native Ecoflex possess two weak reflexes in the 2θ range of 17.7° and 25° as well as two relatively sharp one at around 20° and 23.4° (Fig. 4b). The extruded blend presents only the reflection of the Ecoflex and a lack of a crystalline PLA phase (Fig. 4c). After drawing of the extruded bristles, one pronounced peak in the 2θ range of 16.6° is visible which corresponds to the appearing crystalline PLA fraction (Fig. 4d). As already mentioned, this is due to a stress inducing crystallization of the PLA during stretching of the extruded blend bristles (Fig. 4b). After compression molding, the reflections of the Ecoflex almost vanish while the ones of the PLA become sharper and narrower (Fig. 4e). As discussed before, this observation can be explained by the displacement of the Ecoflex reflections in the meridian direction after compression molding (Fig. 3c) as well as an improvement of the perfection and size of the PLA crystals due to the additional isothermal annealing during hot pressing at 140°C .

Summarizing the WAXS results one can note that in the present case one observes the situations (and changes during manufacturing and processing steps) that are already well documented for MFCs based on polyesters and polyolefins [4–9, 40–45]. These are: (i) a lack of orientation immediately after extrusion, (ii) perfect orientation after cold drawing (necking), (iii) perfection of the crystalline structure of the PLA fibrils, and (iv) regeneration of the isotropic state of the Ecoflex matrix and formation of crystalline regions around the fibrils after the compression molding process. If these regions can be really considered as transcrystalline regions around the PLA fibrils, could not be identified with the methods we used so far. Here, a technique successfully applied by Xu et al. [46] for the study of shish-kebab structures in biodegradable polymers could be of help in the future.

Morphology of the materials

While the WAXS analysis offers information about the crystalline order and orientation of the macromolecules, the microscopic observations can give an idea about the topography and morphological characteristics of the materials.

Scanning electron micrographs of the sample under investigation are shown in Fig. 5. These specimens were prepared by fracturing them in liquid nitrogen perpendicular to the specimen axis. It should be noted that the samples behaved differently during the fracturing, suggesting different morphologies of the blends studied. While

the extruded and compression-molded blends broke exactly perpendicularly to the bristles axis, the as-drawn ones splitted along the drawing direction. The SEM pictures of these samples were taken precisely from these surfaces.

The SEM images of the as-extruded PLA/Ecoflex blend present a distinct two-phase isotropic morphology. Figure 5a, b shows that the PLA is uniformly dispersed in an Ecoflex surrounding in the form of a large number of spherical particles (droplets) with a diameter of $0.5\text{--}1.5\ \mu\text{m}$. Holes of the same shape and size are also observed. It can be concluded that the latter result from the pullout of PLA droplets during cryogenic fracture.

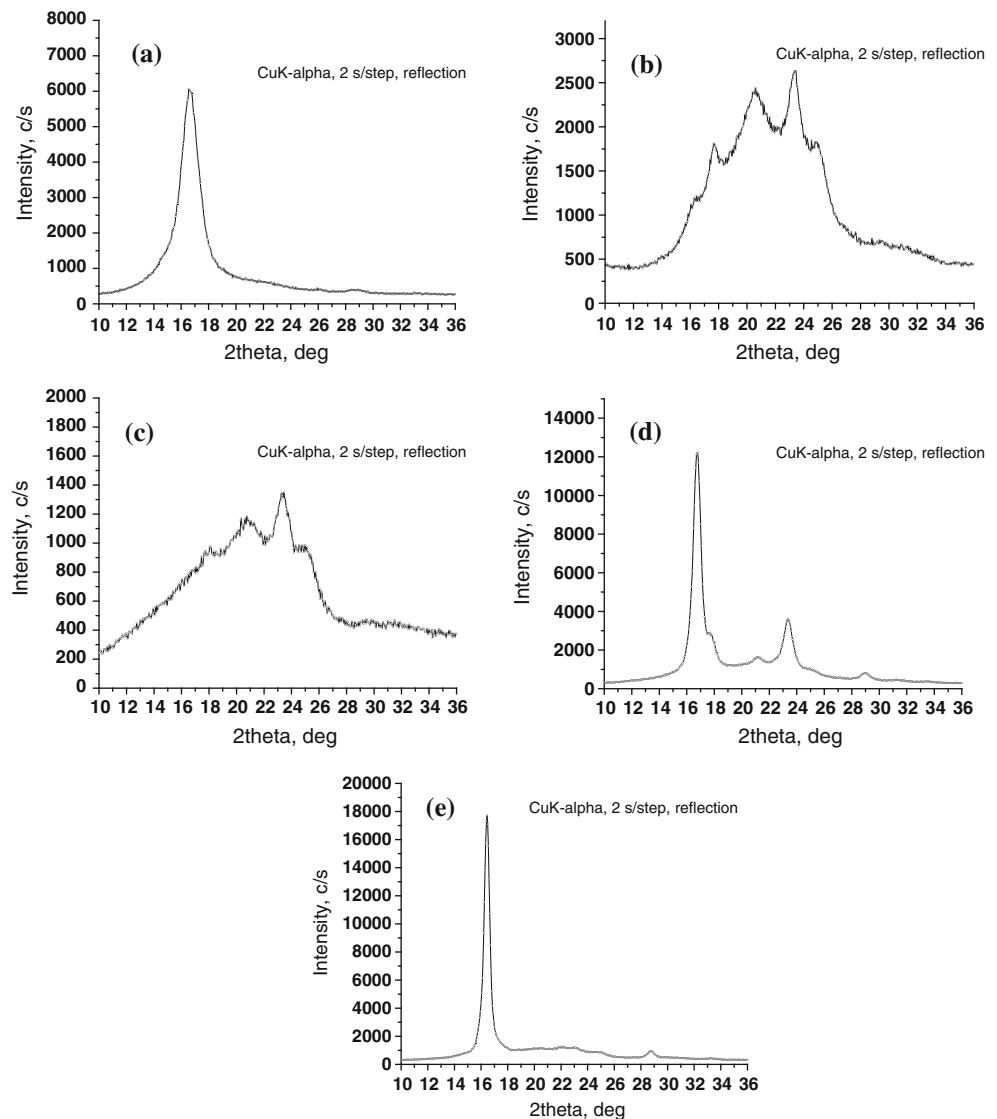
Subsequent drawing results in drastic changes in the blend morphology. As seen from Fig. 5c, d, the fracture surfaces of the as-drawn blend, PLA fibrils with diameters of $0.2\text{--}1\ \mu\text{m}$ were generated during drawing. These morphologies represent highly oriented blends but not a real composite material (in the sense of fibers in an isotropic matrix). From the images one can conclude that the PLA fibrils are distinguished by an extremely high aspect ratio, i.e., the length to diameter ratio, a fundamental importance for all composite materials.

To generate PLA fibrils with nano- or micro-size diameters and a large aspect ratio, drawing of the extrudate is the most critical step. In the heating chamber, where temperature was kept at about 70°C (above T_g of the blend constituents), necking occurred to the extrudate upon drawing and the extrudate was elongated. Consequently, the dispersed PLA particles in the extrudate transform into fibrils through the end-to-end coalescence of the contacting elongated particles. The diameter and the length of the fibrils depend on the amount and the size of the coalescing droplets. It should be noted that the exact or average aspect ratio of the PLA fibrils cannot be correctly determined. This is because one cannot see the entire length of the individual fibrils by SEM observations.

After hot pressing at 140°C where Ecoflex is completely molten, but where the morphologic fibrils are now embedded in a significantly isotropized Ecoflex matrix. As a final result, a composite-like structure is observed (Fig. 5e, f). What is of particular importance is the fact that one does not observe bundle-like aggregates of fibrils, i.e., each fibril is individually surrounded by matrix material. In other words, we have a rather good distribution of the nano- and micro-sized reinforcing material in contrast to the cases with many other nanomaterials used for preparation of polymer nanocomposites.

Additional studies regarding the fibrillar size and distribution were also carried out by a combination of SEM (using a back-scattered electrons detector for better material contrast after staining) and TEM. The results are illustrated in Fig. 6a, b, indicating the good separation of the PLA fibrils and the Ecoflex matrix on a high resolution

Fig. 4 WAXS diffractograms obtained from **a** neat PLA, **b** neat Ecoflex, and PLA/Ecoflex (50/50 by wt) blend after **c** extrusion, **d** drawing, and **e** compression molding



scale, their sub-micron-sized fibril diameter, as well as the average long period of the crystalline lamellae in the matrix. But also here, no direct evidence of transcrystallization phenomena could be identified. The long period of the biodegradable matrix is in the range (around 10 nm) as it was also observed by other authors who studied biodegradable poly(butylene succinate) and its copolyesters [47].

Thermal analysis

The DSC results can give some insight into the phase state, phase transition, crystallization phenomena, melting and degree of crystallinity. For this reason such measurements were performed on the as-extruded PLA/Ecoflex blends, on their intermediate (drawn PLA/Ecoflex blend) as well as on their final products (compression-molded sample). Table 1 summarizes the thermal properties of all the materials under investigation, while Fig. 7 shows the DSC thermograms of

the as-extruded, drawn, and CM blends in the heating and cooling mode.

From Fig. 7a it can be seen that the extruded blend possesses two glass transition peaks (T_g) according to those of the neat polymers, i.e., at about 45 and 64 °C. In addition, a crystallization exothermic peak (T_c) of the PLA is visible at 90 °C, and a very weak endothermic peak (T_m) of the Ecoflex exists near to 120 °C. Upon further heating, the PLA component owns two additional melting peaks, i.e., a weak one at 163 °C and a sharp one at 166 °C. This indicates the presence of crystals with different size and perfection in the PLA fraction of the blends. According to Eqs. (2) and (3), the calculated degrees of crystallinity (W_c) of Ecoflex and PLA are 8 and 32 %, respectively.

After drawing, the T_g of the PLA increases by about 10 °C, while the T_c peak of the same component shifts to a lower temperature (by about 10 °C, as compared to the as-extruded sample) (Fig. 7b). Such cold crystallization immediately after

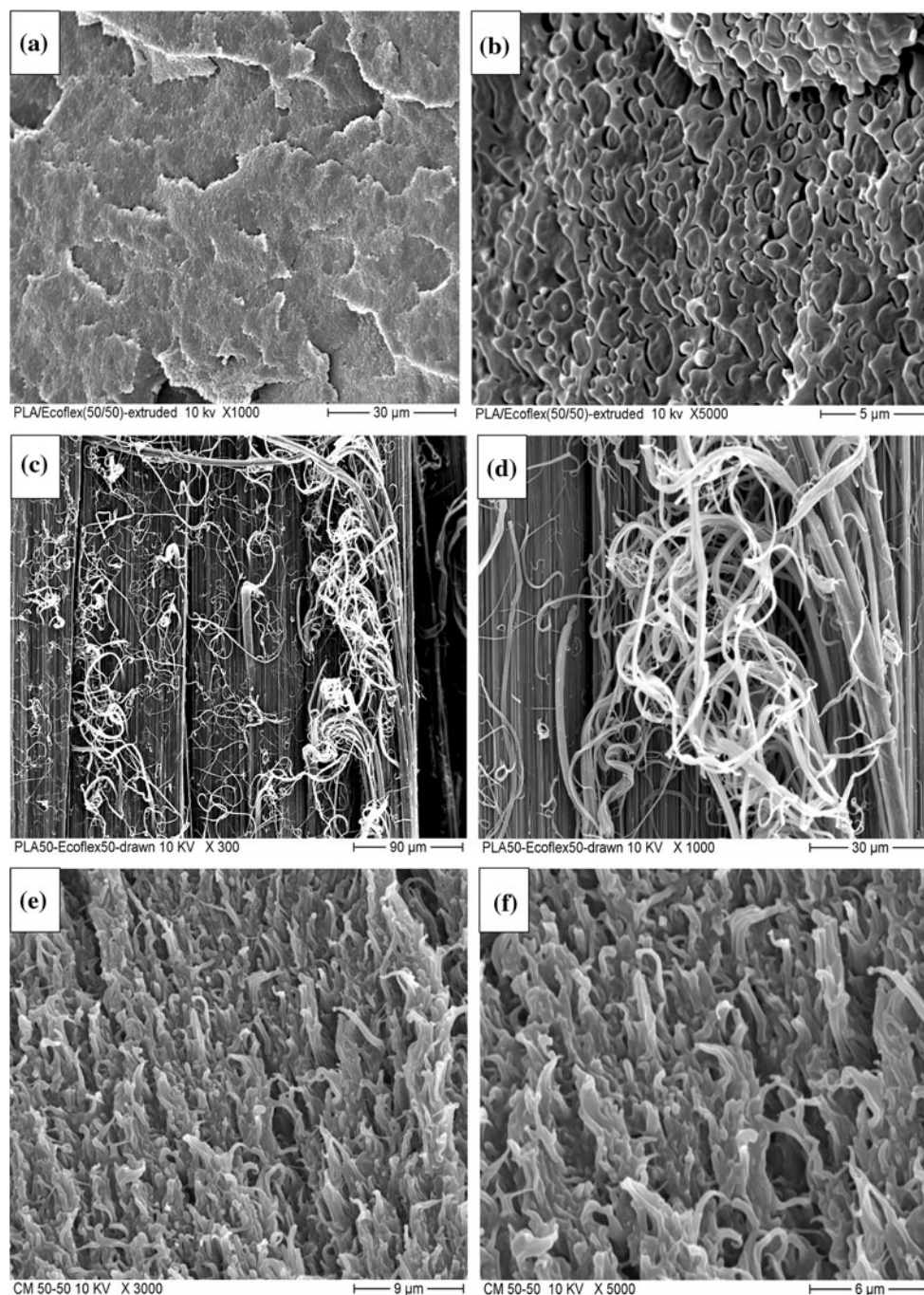


Fig. 5 SEM microphotographs with different magnification of cryogenic-fractured PLA/Ecoflex (30/70 wt%) blends after: extrusion (**a, b**), drawing (**c, d**), and compression molding (**e, f**)

T_g has already been observed for zone-drawn and zone-annealed PET films and fibers [48]. This phenomenon is due to the stretching (fibrillization) and immobilization of the PLA chains in axial direction, which facilitates a crystallization right after the T_g of the polymer. The drawn blend samples possess melting endotherms in the same temperature range as extruded ones. Compared to the crystallinity of the as-extruded

blends, the W_c of the same fractions in the stretched bristles are about 10 % higher (Table 1). These results are in good agreement with the WAXS diffraction photos and diffractograms of the as-extruded and drawn samples, as displayed in Figs. 3 and 4. As mentioned before, this phenomenon is due to stress-induced crystallization and fibrillization of the blend constituents.

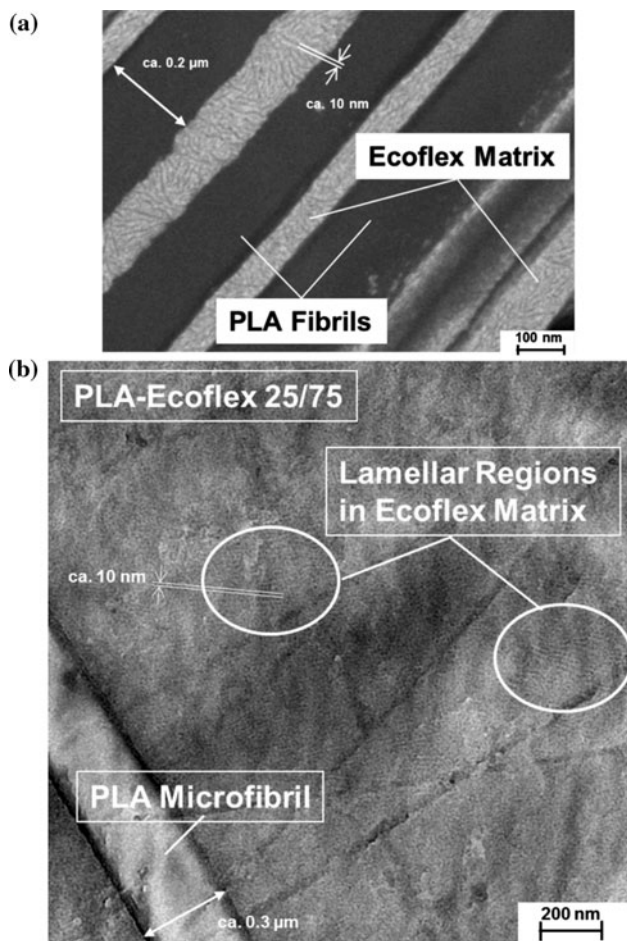


Fig. 6 High resolution SEM image of a blend surface (the flat surface was prepared by cutting with a diamond knife), indicating fibril diameter and crystalline regions of the matrix between the individual PLA fibrils (a), and a TEM image of the crystalline regions in the Ecoflex matrix (b)

In Fig. 7c, d it can also be seen that after compression molding the T_g and T_c peaks of the PLA are missing. Only a melting peak T_m appears at 166 °C. At the same time the crystallinity of PLA increases by about 5 % when compared with the same fractions in the drawn samples. The same phenomenon was observed for the neat drawn and compression-molded PLA at 140 °C (Table 1). One can mention here that the CM procedure represents an additional isothermal annealing (at 140 °C) of the drawn blend with fixed ends. This kind of thermo-treatment contributes to a reorganization of the stretched PLA chains and an elaboration of the crystal structure, even during a short treatment period (here 30 s). These results are again in good agreement with WAXS diffraction patterns and diffraction curves of the drawn and compression-molded samples, as displayed in Figs. 3 and 4.

In a study of Garlotta [37] it was demonstrated that under high stress (during drawing), β crystal orthorhombic structures with chains exhibiting a more extended helical conformation are formed. The PLA β crystals are found to

transform into α crystals when annealed above T_g (in this case during annealing with fixed ends during pressing of the drawn bristles at 140 °C) [37]. Due to the reorganization phenomenon the degree of crystallinity of the PLA fibrils increases up to 48 %, which is about 10 % higher when compared to the same fraction in the drawn strands (Table 1).

Qualitative trends in crystallization ability of the PLA and Ecoflex fractions in the blend can be seen from DSC traces which were recorded during the cooling of the samples from the melt. The experimental data of the cooling traces are summarized in Table 1. Because of the low crystallization capacity of the PLA this polymer does not show any exothermic peak, even as neat material or in the blends during cooling from the melt. On the opposite, due to the higher crystallization ability, independent of the blends composition and treatment, the Ecoflex fraction shows exothermic peaks in the range of 70–74 °C (Table 1). Compared to the T_c and ΔH_c obtained during cooling of the plain Ecoflex, this constituent in the blends possess higher crystallization temperature (about 15 °C) and smaller enthalpy of crystallization (about 7 J/g) (Table 1). This is maybe due to nucleation effect of the PLA and supervene hampering crystals growth of the Ecoflex in the bulk during cooling of the melt blends. These results are over again in agreement with the X-ray diffraction data of the drawn and compression molding samples, display in Fig. 7.

Mechanical properties

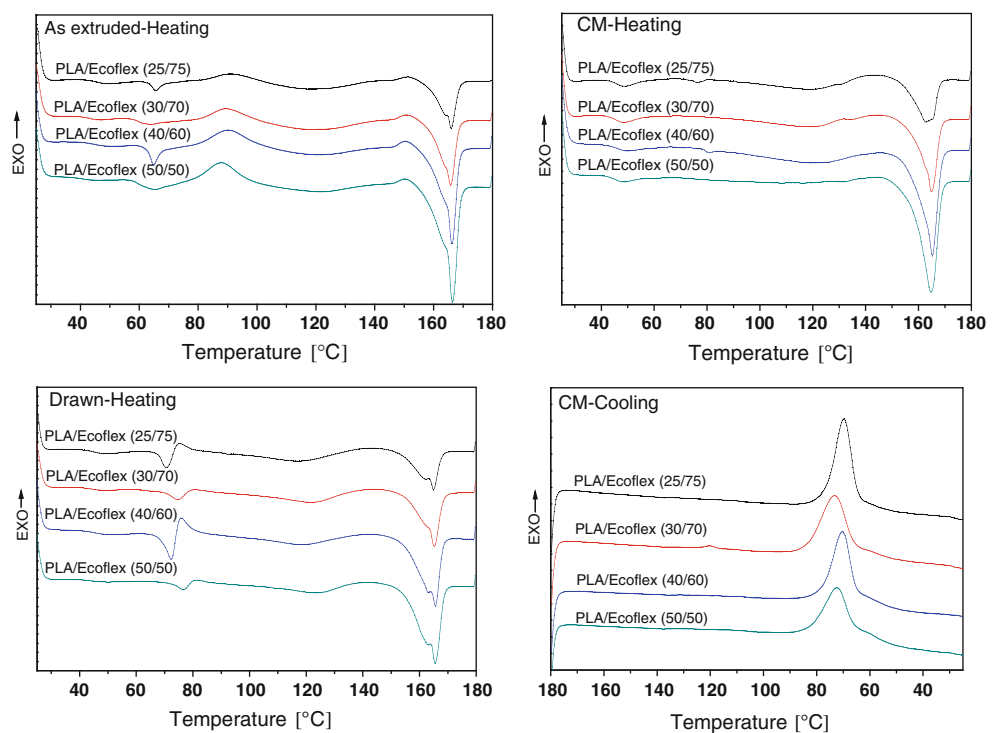
Considering the perfect distribution and excellent aspect ratio of the reinforcing PLA fibrils in the Ecoflex matrix (Fig. 5), one can expect a very high reinforcing efficiency in these polymer–polymer composites. The results of the static mechanical tests of the blends after various stages, together with data for the neat components, are shown in Fig. 8 and summarized in Table 2. First of all, it should be noted that the lowest values of Young’s modulus (E) and tensile strength (σ) were obtained with samples taken immediately after extrusion (Fig. 8). Cold drawing resulted in an abrupt increase of the E and σ values for the all samples under investigation. The modulus of the drawn blends was about 3 times higher, depending on the proportions in the blends, compared to those of as-extruded ones (Fig. 8). This holds also for the values of the tensile strength at break, where the respective differences were up to 7 times greater (Fig. 8; Table 2).

Hot pressing of the drawn blends at 140 °C (isotropization of the Ecoflex) resulted in a drop of the modulus and strength, in accordance with the expectation. Depending on the blend composition, the reduction of the strength was about 1.5–2 times, and of the modulus a bit less (only 7–18 %). At the same time the compression-

Table 1 Thermo-physical properties of the neat PLA and Ecoflex as well as of blends of them with different weight ratios

Sample	T_g (°C)		T_c (°C)	$\Delta H'_c$ (J/g)	T_m (°C)		$\Delta H'_m$ (J/g)		W_c (%)		T_c^* (°C)	$\Delta H'_c$ (J/g)
	Eco	PLA	PLA	PLA	Eco	PLA	Eco	PLA	Eco	PLA	Eco	Eco
PLA												
Extruded	–	63	106	26	–	164	–	–34	–	8	–	–
Drawn	–	65	80	3	–	165	–	–43	–	43	–	–
CM	–	–	–	–	–	166	–	–42	–	47	–	–
Eco CM	45	–	–	–	120	–	–12	–	11	–	55	21
PLA/Eco(25/75)												
Extruded	46	64	91	12	120	163...166	–8	–40	7	31	71	15
Drawn	45	70	78	5	119	162...166	–9	–40	8	41	70	17
CM	46	75	–	–	120	163...165	–7	–40	6	46	70	16
PLA/Eco(30/70)												
Extruded	47	63	90	13	119	164...166	–8	–43	7	32	73	16
Drawn	47	72	82	4	121	162...165	–9	–43	8	43	73	17
CM	46	–	–	–	120	165	–6	–43	5	48	74	16
PLA/Eco(40/60)												
Extruded	46	64	90	15	121	162...166	–10	–45	9	32	71	15
Drawn	46	72	79	7	120	162...166	–9	–45	8	42	71	15
CM	47	73	–	–	120	166	–8	–46	7	49	70	16
PLA/Eco(50/50)												
Extruded	46	64	89	14	122	163...166	–12	–44	9	32	72	14
Drawn	46	71	81	4	123	162...166	–11	–42	9	41	73	16
CM	45	–	–	–	123	166	–6	–45	5	48	72	16

* After cooling mode

Fig. 7 DSC thermograms of the as-extruded, drawn, and compression-molded PLA/Ecoflex blends in heating and cooling mode

molded samples possessed a 25- to 40-time higher modulus as well as a 4.5–8 better tensile strength, when compared to the neat Ecoflex matrix (Fig. 8; Table 2).

Concerning the effect of the blend composition on the mechanical properties, one can conclude that the blends which are richer in PLA reveal the highest E and σ values at each stage of MFC manufacturing. Another interesting observation is that the calculated values [according to Eqs. (4), (5)] of modulus and strength of the hot pressed films (i.e., after isotropization of the Ecoflex fraction in the drawn blends) are almost the same

than the experimentally obtained ones (Fig. 8; Table 2). The experiment values of the Young modulus (6.1 GPa) and the tensile strength (181 MPa) of the neat PLA after drawing and hot pressing at 140 °C were obtained in the present study (Table 2). The tensile modulus and strength of the compression-molded isotropic Ecoflex were found to be 0.08 GPa and 14 MPa, respectively. The almost equal experimental versus calculated values of E and σ could mean that some synergetic effects must be involved, exceeding the properties expected from the rule of mixtures approach.

Fig. 8 Static tensile properties of neat Ecoflex and as-extruded, as-drawn, and compression-molded PLA/Ecoflex blends with different wt ratio. Calculated according to Eqs. (4) and (5) average values are also presented

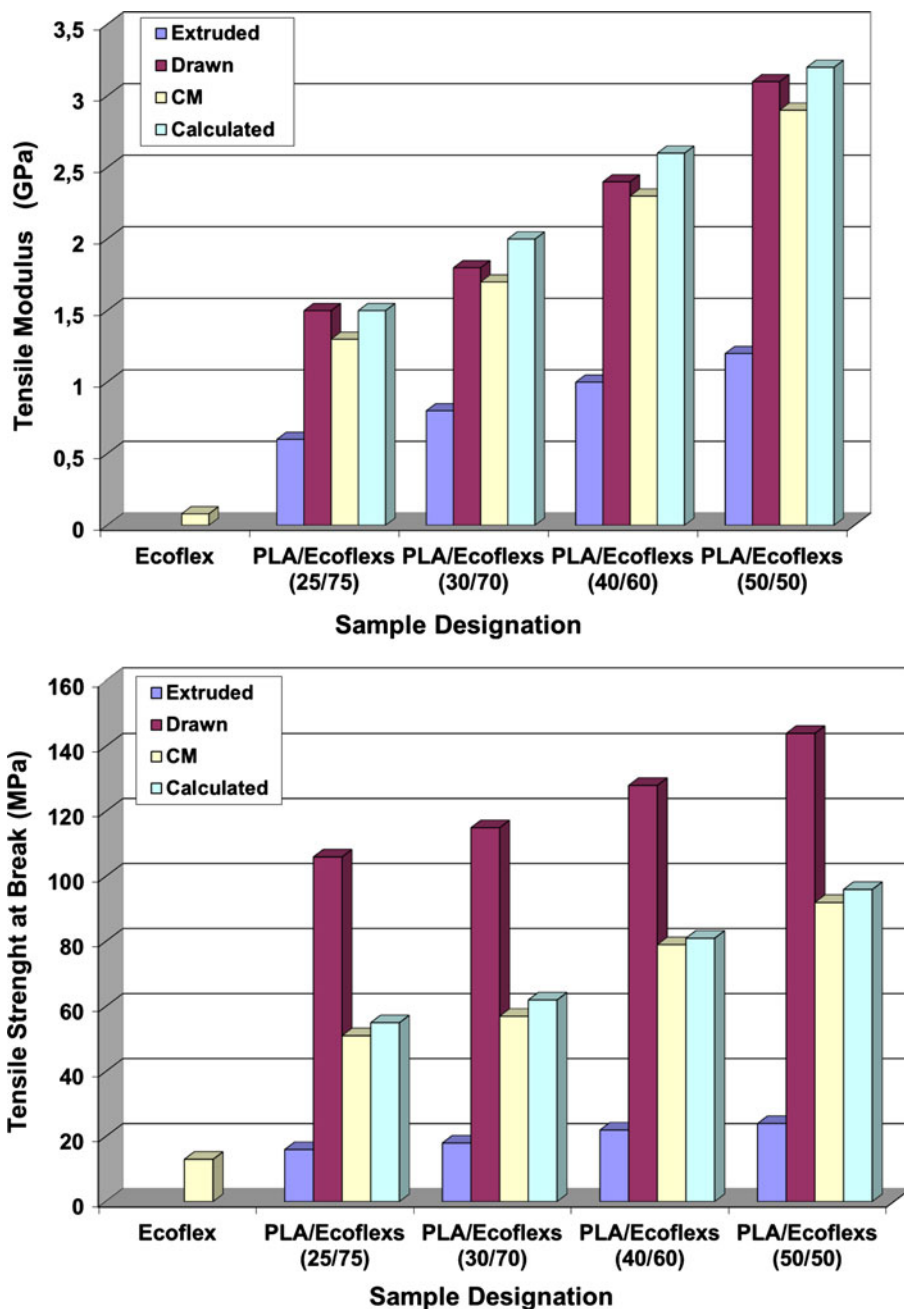


Table 2 Mechanical tensile properties of the neat polymers as well as extruded, drawn, and compression-molded PLA/Ecoflex blends with different weight ratio

Sample	Tensile modulus (GPa)			Tensile strength at yield point (MPa)			Tensile strength at break (MPa)			
	Extruded	Drawn	CM	Extruded	Drawn	CM	Extruded	Drawn	CM	
										Calculated
PLA	2.5	6.6	6.1	40	150	100 (43)*	–	181	180 (57)*	–
PLA/Eco 25/75	0.6	1.5	1.4 (1.6)*	16	32	25 (25)*	30	106	51 (31)*	55
PLA/Eco 30/70	0.8	1.8	1.7 (2.1)*	18	40	30 (23)*	34	119	57 (37)*	62
PLA/Eco 40/60	1.0	2.5	2.4 (3.1)*	21	58	45 (39)*	47	125	81 (49)*	94
PLA/Eco 50/50	1.2	3.1	2.9 (3.3)*	23	63	49 (44)*	53	148	92 (58)*	95
Ecoflex	–	–	0.08 (0.08)*	–	–	7 (6)*	–	–	14 (13)*	–

* Compression-molded plates

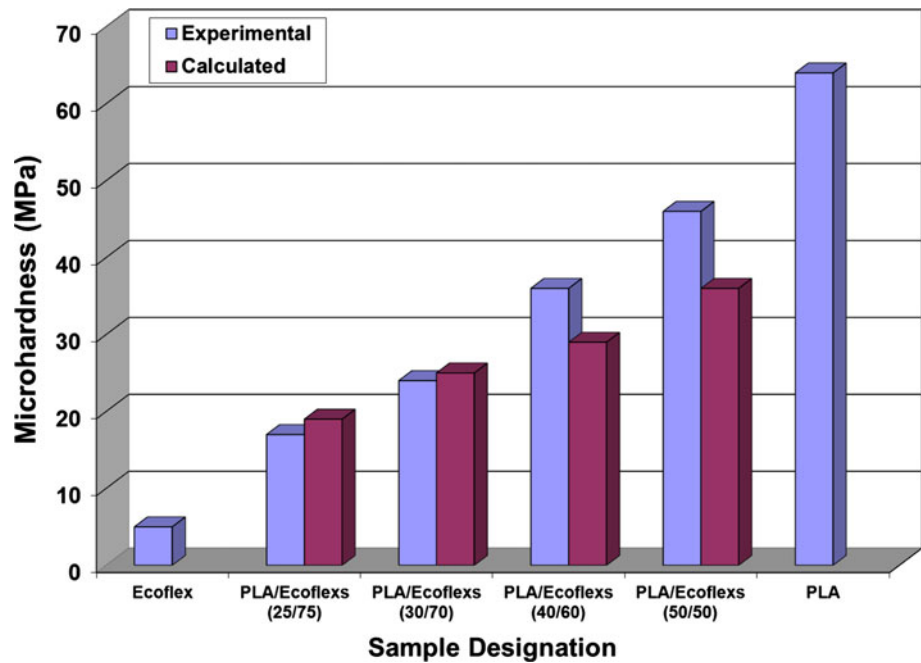
The experimental results described above clearly demonstrate the structure–property relationships of the MFC-structured PLA/Ecoflex blends. In particular, they illustrate the strong reinforcing effect of the PLA fibrils on the mechanical behaviors of the MFC-structured blend materials. Further, the transcrystallization of the matrix polymer onto the surface of the PLA microfibrils provokes an improvement of the adhesion between the blends constituents.

The microhardness properties of the neat polymers and the PLA/Ecoflex compression-molded films (as measured at room temperature), are presented in Fig. 8. A step-like grow-up of the microhardness with an increase of the PLA content in the blend is observed. Compared with the neat Ecoflex, the microhardness of the films rises by 4–12 times for the 25/75 and 50/50 blends, respectively. Because of the stiffness of the PLA it possesses higher microhardness values (by 20–30 MPa, depending of the blend composition) than the compression-molded neat Ecoflex samples (Fig. 9). At the same time, a synergetic effect has been achieved for all samples, if one calculates the microhardness according to Eq. 5 (the rule of mixtures approach), in which for σ the values of the neat polymers are used (Fig. 9). The calculated microhardness of the 40/60 and 50/50 blends are higher than the experimental ones. This illustrates the strong reinforcing effect and the role of the amount of the PLA fibrils, which should be much stronger than the isotropic PLA. Unfortunately the exact microhardness of the individual microfibrils cannot be determined, because of their small diameter (in the range of 0.15–1.5 μm).

The mechanical properties of the compression-molded strip-like samples (films) after artificial aging at a relative humidity of 50 %, a chamber temperature of 50 °C, and a treatment period of 10, 20, or 30 days are presented in Fig. 10. In accordance with the expectations, a step-like drop of the tensile modulus and strength of the samples with increasing treatment duration is observed. Depending on the blend composition, the reduction of the modulus amounts to 0.5–0.7 GPa, while the drop of the strength is in the range of 15–20 MPa after 30 days of treatment. This may be due to the strong influence of the ultraviolet irradiation and the temperature on the Ecoflex matrix. Because of the chemical composition of this three components copolymer (poly(butylene adipate-co-terephthalate) its resistance diminishes under such conditions. It is logical to assume that, as a result of tearing of covalent bonds followed by their fragmentation (destruction), the Ecoflex matrix is destroyed. This degradation process provokes the formation of cavities and cracks at the Ecoflex/PLA interphase and the debonding of the PLA fibrils from the matrix (Fig. 10).

The producer of Ecoflex (BASF) declares that this polymer is fully biodegradable (according to EN 13432, part 2). Its degradation elapses for about 80 days, and more than 90 % of the polymer is converted into CO₂, water,

Fig. 9 Microhardness properties of neat Ecoflex and compression-molded PLA/Ecoflex blends with different wt ratio



and energy biomass, as a result of irradiation and microorganisms impact [19]. In this investigation, microorganisms were not used, so that a drastic degradation of the matrix did not start before 30 days of exposure. The reason for the observed better mechanical behavior of the aged blend samples, in comparison to the virgin, non-aged Ecoflex (Fig. 10), is the reinforcing contribution of the PLA fibrils as well as the transcrystallization phenomenon. This is independent of the fibrils–matrix phase separation during artificial aging of the composites. It should be noted also that PLA fibrils are much more resistant to degradation under aging conditions, because of their chemical composition, their higher T_g (above 75 °C), and their relatively high crystallinity in the blends (about 48 %) (Table 1).

The tensile properties of the compression-molded (140 °C) PLA/Ecoflex plates with different compositions are summarized in Fig. 11 and Table 2. The flexural modulus of all blends increases step-like with the rise of the PLA content in the blends, reaching maximal values, being about 2,000 % (for the 25/75 blend) and 4,000 % (for the 50/50 blend) higher than those of the neat Ecoflex (Fig. 11; Table 2). The same trend is observed for the flexural strength. With the rise of the LCP fraction in the blends the strength increases up to 200 % (for the 25/75 blend) and 400 % (for the 50/50 blend). On the other hand, one can see from Table 2 and Fig. 11 that the modulus and strength of the PLA/Ecoflex (50/50 by wt) samples possess almost the same values as the compression-molded neat PLA.

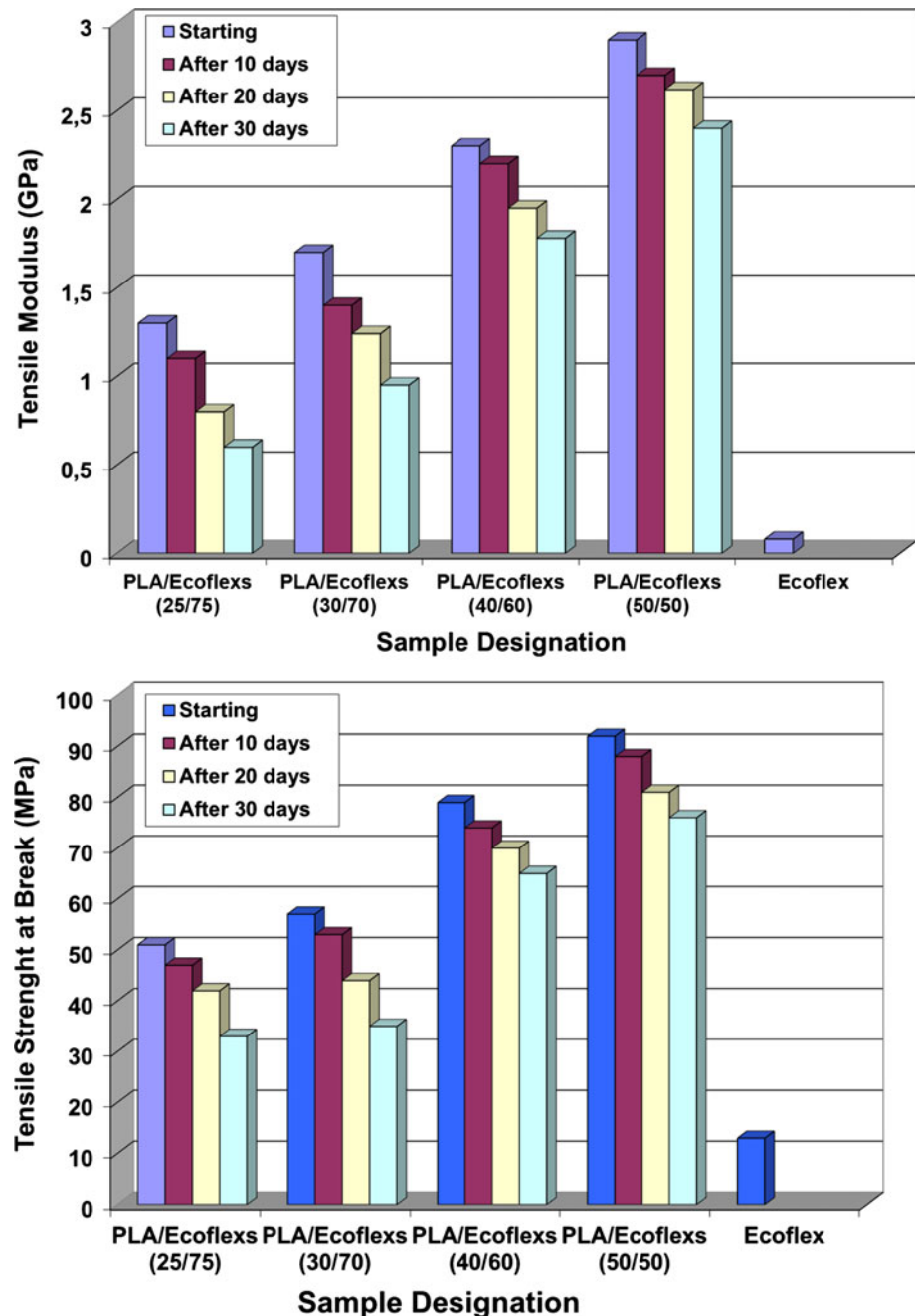
It should be mentioned here that depending on the blend compositions, the mechanical properties obtained for the compression-molded plates are much higher (200–400 %

in case of Young's modulus and 240–440 % in case of strength) than those of neat Ecoflex. According to Bousmina [48], only in exceptional circumstances one can observe an improvement in the mechanical performance of nanocomposites of greater than 30 %, including their barrier properties [49–51].

In order to clarify the fracture mechanisms responsible for the improved mechanical properties, the tensile fracture parts of the broken flexure surfaces of compression-molded PLA/Ecoflex samples and neat Ecoflex were observed by SEM (Fig. 12). As Ecoflex can be considered as a ductile polymer, it is obvious to expect a great amount of plastic deformation on the fractured surface due to stretching and subsequent failure of the matrix at about 400 % deformation (Fig. 12a). PLA fibrils in such samples showed, on the other hand, no necking in the tensile test region, but a smooth fracture surface without visible plastic deformation (Fig. 12b). Cavities and cracks along the PLA fibrils as well as debonding of the Ecoflex matrix from the PLA fibrils under tensile stress are also clearly visible (Fig. 12c, d). These cavities and cracks were formed during tension when the stress was higher than the bonding strength of the interface between the PLA fibrils and the Ecoflex matrix. The cavities were enlarged in the stress direction along with a deformation of the Ecoflex matrix.

Since PLA has different elastic properties compared to the Ecoflex matrix, its fibrils act as stress concentrators under tensile stress. The stress concentration gives rise to high triaxial stresses in the material. From the literature it is well known, that in a blend-containing rubber-toughened polymer materials, there exist two types of cavitations:

Fig. 10 Static tensile properties of neat Ecoflex and compression-molded PLA/Ecoflex blends with different wt ratio subject to artificial aging



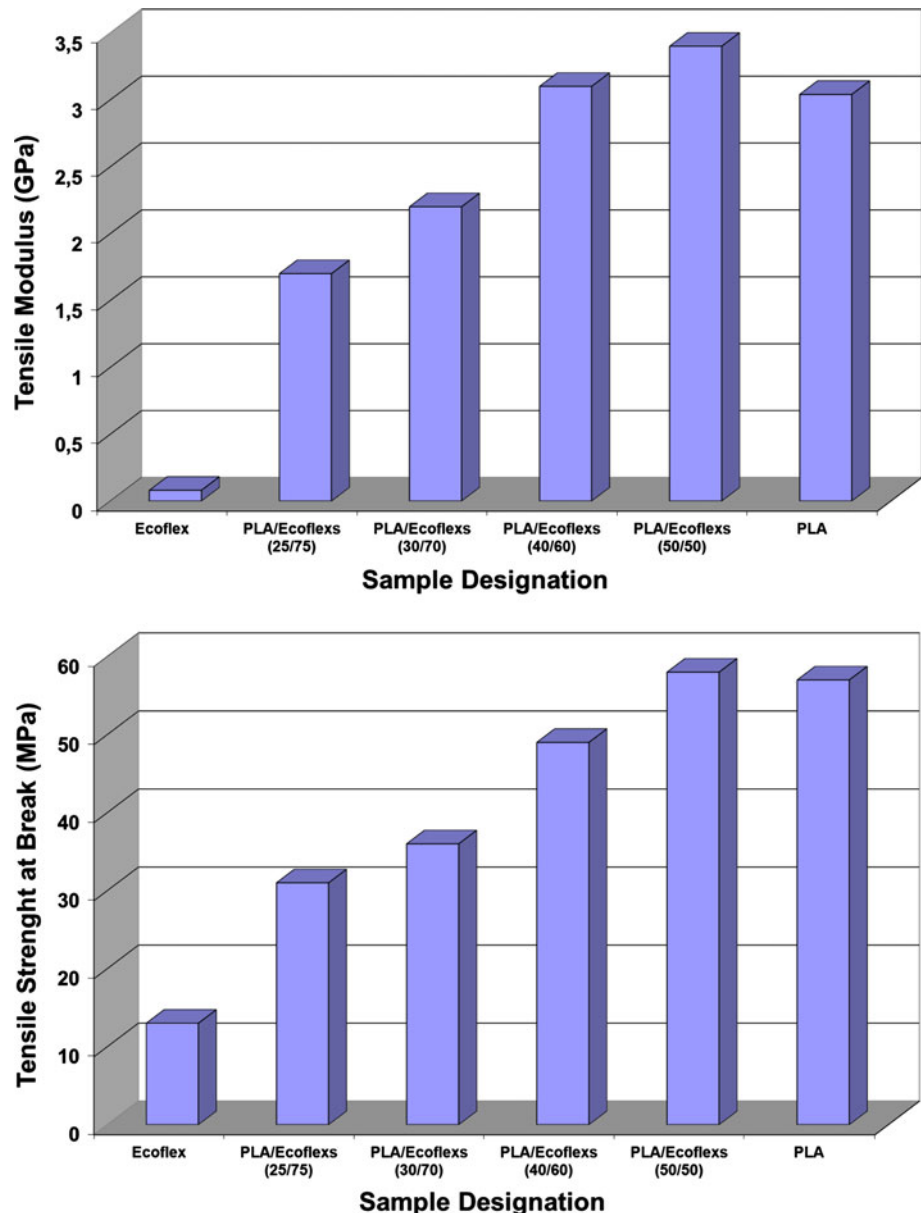
(i) either formation of holes within the rubber inclusions, as long as there is a strong interfacial bonding between the blend components and a relatively weak strength of the rubber phase itself, or (ii) at the interface, when the interfacial bond strength is lower than the strength of the rubber particles in the polymer matrix. Because in the present case there was not enough sufficient interfacial adhesion between the Ecoflex matrix and the PLA reinforcement, interfacial debonding took place (instead of cavitation within the Ecoflex core under the triaxial stress). With such a progress of debonding, the rubber-like matrix could

deform more easily and resulted in a high contribution of shear yielding.

Barrier properties

The rate of penetrating gas through a polymeric material is determined by the following factors: (i) the penetrant's solubility in the polymer, (ii) the relationship between the size of the penetrating gas molecule and the interstices in the polymer, and (iii) the temperature and humidity [52]. Barrier property differences occur, because of the

Fig. 11 Static tensile properties of compression-molded Ecoflex and PLA as well as PLA/Ecoflex palates with different blend composition



enormous variations in molecular structure and chain distribution possible between different types and grades of polymer. Blend morphology in multi-phase systems influences the diffusion paths available to penetrating molecules, as does the degree of branching and cross-linking, the structure of the monomer units, and the level of free volume present [52, 53]. Permeability of a polymer composite system to gases or liquids needs special consideration, include aspect ratio, orientation and dispersion of the filler, as well as its shape, dimensions and volume fraction, the density and crystallinity of the matrix, and the affinity between the constituent polymers and the diffusing species [54, 55]. Concerning the influence of the matrix crystallinity on the permeability, it should be noted that the amorphous regions tend to be easier for molecules to

permeate through when contrasted with tightly packed crystalline regions [56].

Oxygen permeability results for compression-molded MFC-structured PLA/Ecoflex plates (25/75 and 50/50 wt%) as well as plain, compression-molded PLA, and Ecoflex samples are shown in Fig. 13. It is evident that the plates have considerably enhanced oxygen barrier properties when compared to the plain Ecoflex. The blend plates have almost two times (for 25/75 blend composition) and about 5 times (for 50/50 samples) less oxygen permeability than the neat Ecoflex. This indicates clearly the potential to improve neat Ecoflex for oxygen barrier applications. In addition, the oxygen transmission rate of the 50/50 samples is almost equal to the neat PLA behavior (Fig. 13). These tests confirm that the conditions used for

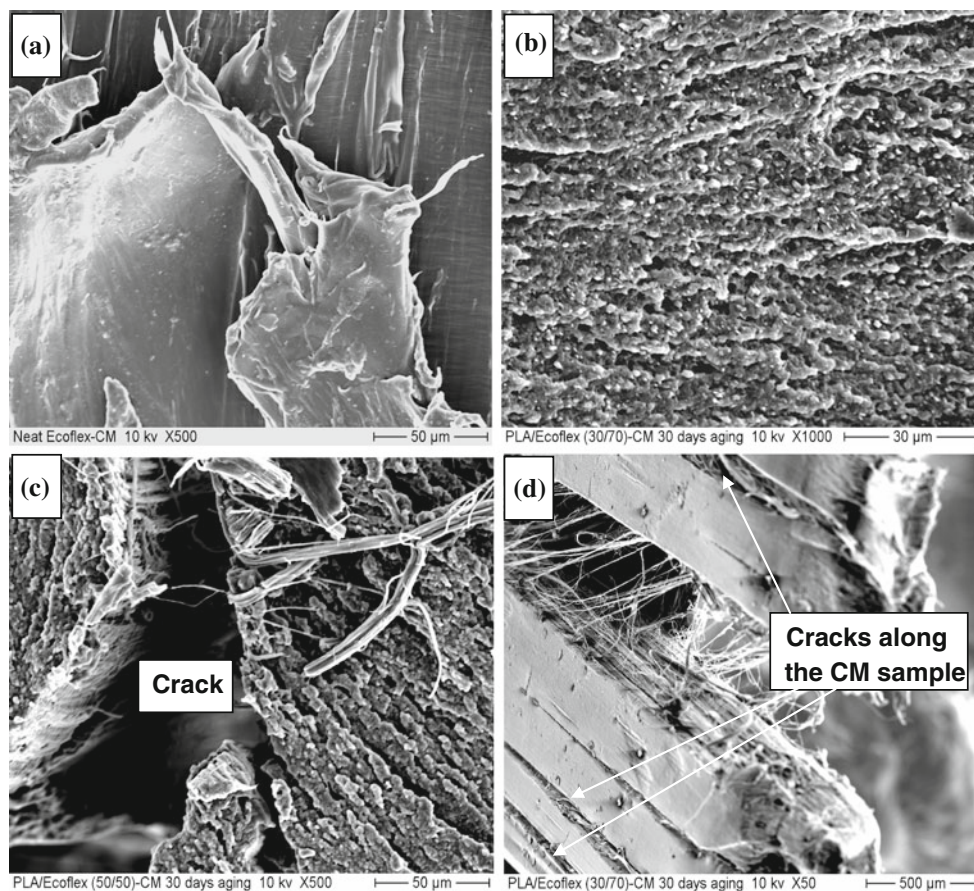
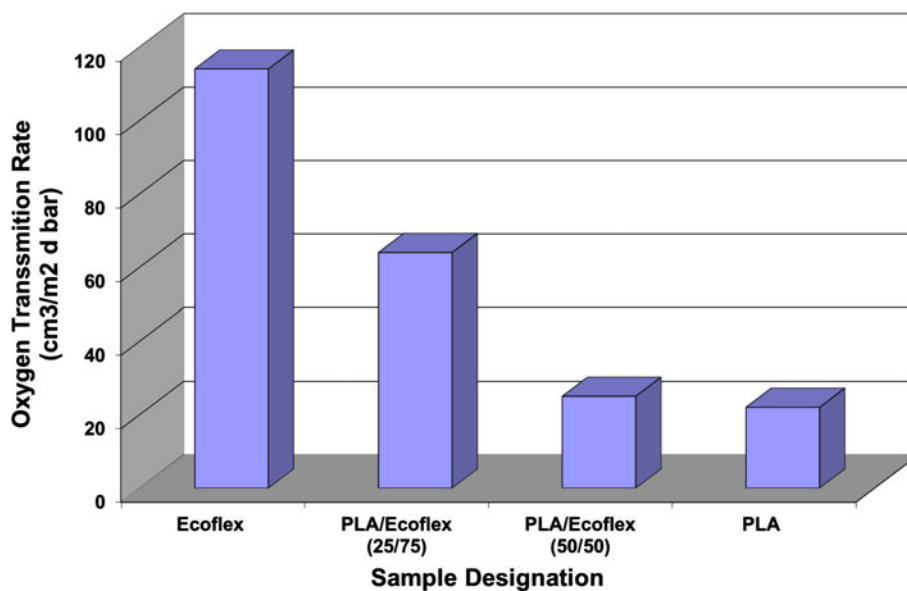


Fig. 12 SEM microphotographs of tensile fractured compression-molded at 140 °C samples **a** surface of neat Ecoflex, **b** surface of PLA/Ecoflex (30/70 wt%), **c** surface of PLA/Ecoflex (50/50 wt%), and **d** photo of the PLA/Ecoflex (30/70 wt%) fractured sample

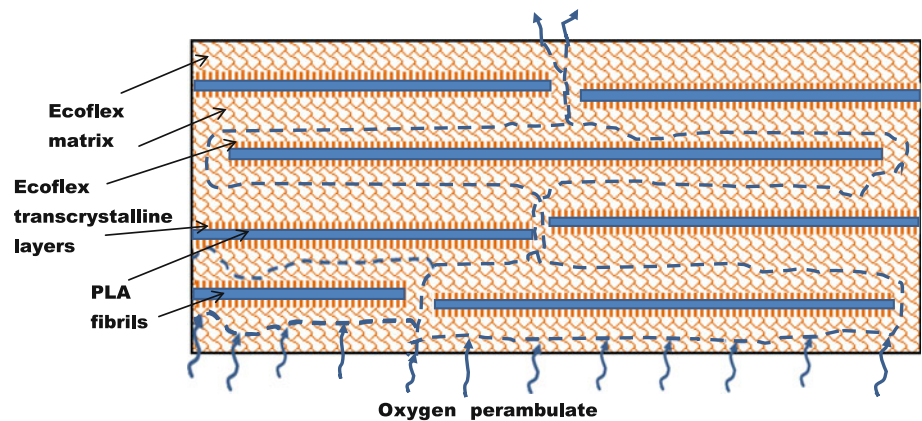
Fig. 13 Oxygen transmission rate of compression-molded PLA/Ecoflex palates and homopolymers



manufacturing MFC materials (both during the initial extrusion steps as well as after the compression molding process) contribute significantly to their permeability

characteristics through alteration of the reinforcing phase geometry. The samples with the lowest permeability (50/50 samples) had tripled the oxygen barrier effectiveness of the

Fig. 14 The distance a penetrating molecule must travel to permeate a polymer composite is influenced by the internal morphology of the composite. The volume, form, and the length of the filler create greater distances, which result in lower permeability



25/75 specimen (Fig. 13), despite the fact that both were produced using the same polymer components. This indicates the necessity to determine the nature of the relationship between permeability and morphology of the samples in more detail. It is logical to assume that the 50/50 plates possess at least two times more volume fraction of PLA fibrils, when compared with the 25/75 samples, which increases the path of the penetrating gas. If one invokes a tortuosity argument that the permeability of a material is directly influenced by the length of the path that the penetrating gas must travel during transit, and thus a longer path reduces permeability, it becomes immediately obvious why MFC compression-molded samples should exhibit enhanced barrier properties (Fig. 14).

Conclusions

From the results and discussions in this paper the following conclusions can be deduced:

- MFC structures can be successfully achieved with biodegradable PLA/Ecoflex blends, using an industrially relevant line, i.e., by melt extrusion followed by continuous cold drawing of the extrudates, and a subsequent isotropization step of the polymer matrix.
- Strip-like specimens (films) and plates (laminates) were prepared by compression molding (CM) of the drawn blends at processing temperature above the melting temperature (T_m) of the Ecoflex and below T_m of the PLA.
- The SEM observations show a high level of orientation, a high aspect ratio, and a small diameter of the PLA fibrils (150 nm–1.5 μ m). Besides, a perfect distribution of the fibrils in the Ecoflex matrix and a complete absence of fibrillar aggregates after compression molding processing were observed.
- By means of WAXS it was indicated that a formation of anisotropic layers of the Ecoflex matrix on the surface of the PLA microfibrils takes place. In these layers, the

crystalline lamellae arise during non-isothermal crystallization from the melt and are aligned parallel to each other. The PLA fibrils not only promote the crystallization, but they also affect the orientation of the matrix chains during the transcrySTALLIZATION. This is in contrast to the bulk matrix where the lamellae are quasi-randomly arranged. The self-assembled structure plays the role of a “physical compatibilizer” and improves the adhesion between the fibrils and the matrix.

- A comparison of the mechanical properties and the oxygen barrier behavior of the MFCs created during this investigation confirmed significant improvements in both areas. Depending on the blend compositions, the compression-molded samples possessed a 2.4- to 4.4-time higher tensile strength as well as a 20–40 % better modulus than the neat Ecoflex. A similar trend was settled for the microhardness properties of the same specimens.
- Permeation results have shown that significant barrier improvements can be attained with a microfibrillar structure. The compression-molded plates have been shown to possess superior oxygen barrier properties compared to the plain Ecoflex, i.e., the permeability decreases up to 5 times.
- The results are quite encouraging and indicate that there is much potential for MFC-structured PLA/Ecoflex blends to be developed for packaging materials, especially suitable for applications in which Ecoflex is currently the material of choice. Permeation results have shown that significant barrier improvements can be attained with a drawn microfibrillar structured PLA/Ecoflex blend, and that drawing of the blend is paramount if significant increases in tensile strength and modulus are also desired.

Acknowledgements The authors acknowledge the financial support of the Germany DAAD Foundation (Project 54391873), as well as of the Bulgarian Foundation for Research and Science, and Uta Reuter (Leibniz-Institut für Polymerforschung Dresden e.V.) for TEM support.

References

- Paul DR, Bucknall CB (2000) *Polymer blends*, vol 2. Wiley, New York
- Utracki LA (2002) Introduction to polymer blends. In: Utracki LA (ed) *Polymer blends handbook*. Kluwer Academic Publishers, Dordrecht
- Evstatiev M, Fakirov S (1992) *Polymer* 33:877
- Evstatiev M, Fakirov S, Schultz JM, Friedrich K (2001) *Polym Eng Sci* 41:192
- Evstatiev M, Fakirov S, Krasteva B, Friedrich K, Covas J, Cunha A (2002) *Polym Eng Sci* 42:826
- Friedrich K, Kamo H, Evstatiev M, Fakirov S (2004) *J Macromol Sci Phys* 43:776
- Friedrich K, Evstatiev M, Fakirov S, Evstatiev O, Ishii M, Harrass M (2005) *Compos Sci Technol* 65:107
- Fakirov S, Shields RJ, Fuchs C, Friedrich K, Bhattacharyya D (2008) *Int J Polym Mater* 1:33–53
- Shields RJ, Bhattacharyya D, Fakirov S (2008) *Compos A* 39:940
- Ihm DW, Hiltner A, Baer E (1991) In: Baer E, Moet A (eds) *High performance polymers*. Hanser, Munich
- Huang WY, Shen JW, Chen HY (2003) *J Mater Sci Lett* 22:377
- Li ZM, Li BL, Shen KZ, Yang W, Huang R, Yang MB (2004) *Macromol Rapid Commun* 25:553
- Albertsson A-C, Karlsson S (1994) In: Griffin GJL (ed) *Chemistry and technology of biodegradable polymers*. Blackie, Glasgow
- Ali SAM, Doherty PJ, Williams DF (1994) *J Appl Polym Sci* 51(8):1389
- Steinbüchel A (1995) *J Macromol Sci Pure Appl Chem* A32(4):653
- Mohanty AK, Misra M, Hinrichsen G (2000) *Macromol Mater Eng* 276/277:1
- Plackettanda D, Vazquez Z (2004) In: Baillie C (ed) *Green composites*. Woodhead Publishing Ltd/CRC Press LLC, Cambridge/Boca Raton
- Witt U, Einig T, Yamamoto M, Kleeber I (2002) *Chemosphere* 44:289
- BASF (2001) 23/02/01-last update, a news service provided by BASF. Available online
- Sok RM (1994) Permeation of small molecules across a polymer membrane: a computer simulation study. University of Groningen, Groningen, pp 5–12
- Fakirov S, Shields RJ, Fuchs C, Friedrich K, Bhattacharyya D (2008) *Int J Polym Mater* 57(1):33
- Jiang L, Wolcott MP, Zhang J (2006) *Biomacromol* 7:199
- Liu TY, Lin WC, Yang MC, Chen SY (2005) *Polymer* 46:12586
- Lee SM, Lee YJ, Lee JW (2007) *Macromol Res* 15:44
- Gu SY, Zhang K, Ren J, Zhan H (2008) *Carbohydr Polym* 74:79
- Signori F, Coltelli MB, Bronco S (2009) *Polym Degrad Stab* 94:74
- Zhang NW, Wang QF, Ren J, Wang L (2009) *J Mater Sci* 44:250. doi:10.1007/s10853-008-3049-4
- Coltelli MB, Della Maggiore I, Bertold M, Signori F, Bronco S, Ciardelli F (2008) *Appl Polym Sci* 110:1250
- Yeh J-T, Tsou C-H, Huang C-Y, Chen K-N, Wu C-S, Chai W-L (2010) *J Appl Polym Sci* 116:680
- Yuan H, Liu ZY, Ren J (2009) *Polym Eng Sci* 49(5):1004
- Wang RY, Wang SF, Zhang Y (2009) *J Appl Polym Sci* 113(6):3630
- Yang F, Qiu ZB (2011) *J Appl Polym Sci* 119(3):1426
- NatureWorks® PLA Polymer 6202D, Data Sheet (2006)
- Herrera R, Franco L, Rodríguez-Galán A, Puiggali J (2002) *J Polym Sci A Polym Chem* 40:4141
- Shi XQ, Ito H, Kikutani T (2005) *Polymer* 46:11442
- Ou X, Cakmak M (2008) *Polymer* 49:5344
- Garlotta D (2002) *J Polym Environ* 9:63
- Cartier L, Lotz B (2000) *Polymer* 41:8909
- Cicero JA, Dorgan JR, Janzen J, Garrett J, Runt J, Lin JS (2002) *J Appl Polym Sci* 86:2839
- Fakirov S, Evstatiev M, Friedrich K (2002) In: Fakirov S (ed) *Handbook of thermoplastic polyesters: homopolymers, copolymers, blends and composites*. Wiley-VCH, Weinheim
- Evstatiev M, Schultz JM, Fakirov S, Friedrich K (1998) *J Appl Polym Sci* 67:723
- Evstatiev M, Fakirov S, Friedrich K (2000) *Adv Polym Technol* 19:249
- Fakirov S, Evstatiev M, Friedrich K (2002) In: Fakirov S (ed) *Handbook of thermoplastic polyesters*. Wiley-VCH, Weinheim
- Evstatiev M, Fakirov S, Friedrich K (2005) In: Friedrich K, Fakirov S, Zhang Z (eds) *Polymer composites: from nano- to macro scale*. Kluwer Academic Publishers, Nowell
- Evstatiev M, Fakirov S, Apostolov AA, Hristov H, Schultz JM (1992) *Polym Eng Sci* 32:964
- Xu H, Zhong G-J, Fu Q, Lei J, Jiang W, Hsiao B-S, Li Z-M (2012) *ACS Appl. Mater Interfaces* 4:6774
- Gan Z, Abe H, Kurokawa H, Doi Y (2001) *Biomacromolecules* 2:605
- Bousmina M (2005) In: 21st Annual meeting of the polymer processing society (PPS 21), Leipzig, 19–23 June, p 219 (Abstracts book)
- Kee DE, Zhong Y, Zheng Y, Janes D (2005) In: 21st Annual meeting of the polymer processing society (PPS 21), Leipzig, 19–23 June, p 222 (Abstracts book)
- Kalendova A, Peprniecek T, Kovarova L, Hrnčirik J, Simonik J, Duchet J (2005) In: 21st Annual meeting of the polymer processing society (PPS 21), Leipzig, 19–23 June, p 223 (Abstracts book)
- Bismarck A, Mishra S, Lampe T (2005) In: Mohanty A, Misra M, Drzal LT (eds) *Natural fibres, biopolymers, and biocomposites*. CRC/Francis Taylor, Boca Raton
- Gajdos J, Galic K, Kurtanek Z, Cikovic N (2001) *Polym Test* 20:49
- Pino M, Duckett RA, Ward IM (2005) *Polymer* 46:4882
- Massey LK (2003) *Permeability properties of plastics and elastomers—a guide to packaging and barrier materials*. William Andrew Publishing, Norwich
- Mai YW, Wong JSS, Li RKY, Lu C (2004) On the tearing toughness and permeability modelling of polymer nanocomposites. Society of Plastics Engineers, Chicago, pp 1785–1789
- Liu RYF, Hu YS, Schiraldi DA, Hiltner A, Baer E (2004) *J Appl Polym Sci* 94:671